Journal of Magnetic Resonance 222 (2012) 53–58

Contents lists available at SciVerse ScienceDirect

Journal of Magnetic Resonance

journal homepage: www.elsevier.com/locate/jmr

Dual-scan acquisition for accelerated continuous-wave EPR oximetry

J. Palmer [a], L.C. Potter [a], D.H. Johnson [b], J.L. Zweier [b], R. Ahmad [b,*]

[a] Department of Electrical and Computer Engineering, The Ohio State University, Columbus, OH 43210, USA
[b] Davis Heart and Lung Research Institute, Department of Internal Medicine, The Ohio State University, Columbus, OH 43210, USA

ARTICLE INFO

Article history:
Received 2 March 2012
Revised 11 May 2012
Available online 13 June 2012

Keywords:
EPR
Spectroscopy
Oximetry
Overmodulation
Cramér–Rao lower bound
LiNc-BuO

ABSTRACT

Statistical analysis reveals that, given a fixed acquisition time, linewidth (and thus pO_2) can be more precisely determined from multiple scans with different modulation amplitudes and sweep widths than from a single-scan. For a Lorentzian lineshape and an unknown but spatially uniform modulation amplitude, the analysis suggests the use of two scans, each occupying half of the total acquisition time. We term this mode of scanning as dual-scan acquisition. For unknown linewidths in a range $[\Gamma_{min}, \Gamma_{max}]$, practical guidelines are provided for selecting the modulation amplitude and sweep width for each dual-scan component. Following these guidelines can allow for a 3–4 times reduction in spectroscopic acquisition time versus an optimized single-scan, without requiring hardware modifications. Findings are experimentally verified using L-band spectroscopy with an oxygen-sensitive particulate probe.

1. Introduction

Electron paramagnetic resonance (EPR) is a spectroscopic method for the detection of species with unpaired electrons. Long data acquisition times have limited the scope of EPR for biological studies, such as *in vivo* measurements of pO_2 and pH.

For continuous-wave (CW) EPR, the data are collected by measuring the absorption of electromagnetic radiation, usually in the microwave range, by paramagnetic species in the presence of an external magnetic field. For imaging applications, an additional magnetic field in the form of a linear magnetic field gradient is applied to provide spatial encoding. Recent efforts to accelerate EPR data collection include both hardware and algorithm developments. For example, overmodulation [1], fast scan [2], rapid scan [3,4], pulsed EPR [5,6], parametric modeling [7], adaptive and uniform data sampling [8], digital detection [9–11], and multisite oximetry [12,13] have shown potential to accelerate the acquisition process.

To improve signal-to-noise ratio (SNR), magnetic field modulation is universally employed in CW EPR [14]. To increase signal strength, the magnetic field modulation amplitude (B_m) is often set to three or four times the half-width half-maximum (HWHM) linewidth (Γ) expected to be measured in the experiment. In previous work, we have demonstrated how to set B_m and the sweep width (Δ_B) for increased sensitivity when performing a single-scan [15].

In this study we ask the following question: can a fixed scan time be split into multiple scans with various modulation amplitudes and sweep widths to provide more informative measurements than a single-scan? By way of analogy, what can we gain by examining this spectral object from multiple perspectives? Our primary investigative tool is the Cramér–Rao lower bound (CRLB). Given a candidate number of scans R, the time for each scan, and the settings for each scan, the CRLB allows us to determine how well the linewidth, Γ, can be estimated. The provided bound is on the standard deviation (std.) of the estimation error: no unbiased estimator can perform better than this.

The remainder of the paper is organized as follows: Section 2 presents the signal model and the statistical sensitivity analysis used to optimize acquisition parameters; Section 3 briefly describes the construction of the phantom as well as the protocols used to collect data on an L-band spectrometer; Section 4 presents results from both simulation and L-band oximetry experiment; Section 5 includes discussion; and Section 6 summarizes the conclusions.

2. Theory

2.1. Signal model

Our analysis relies on the following assumptions: (i) the value of Γ is unknown, but resides in a known range $[\Gamma_{min}, \Gamma_{max}]$; (ii) signal intensity d is unknown; (iii) the nth scan's modulation amplitude ($B_{m,n}$) is unknown, but constant over the extent of the sample; (iv) the center field of the lineshape is known; (v) the sweep rate is low enough to avoid the rapid-scan regime [3]; (vi)

* Corresponding author. Address: 420 W 12th Ave., Suite 126A, Columbus, OH 43210, USA. Fax: +1 614 292 8454.
E-mail address: rizwan.ahmad@osumc.edu (R. Ahmad).

1090-7807/$ - see front matter © 2012 Elsevier Inc. All rights reserved.
http://dx.doi.org/10.1016/j.jmr.2012.05.021

measurement noise is additive white Gaussian [7]; and (vii) the lineshape is a modulation-distorted Lorentzian, as detailed below.

Note that each modulation amplitude, B_m, though nominally set by the experimenter, is considered unknown. This is because the actual B_m values vary slightly but unpredictably from the set value. Also note that we have assumed the center field of the lineshape is known. In many situations, the center field may vary slightly between scans or not be properly calibrated; numerical study as well as lab experiments (not shown) indicate that small center field offsets do not significantly affect our results.

Our signal model for the modulation-distorted Lorentzian lineshape is adapted from Robinson et al. [16] and has previously proven effective in EPR oximetry [1,15]. Because the linewidths encountered in EPR oximetry are large compared to the ratio of the modulation frequency to the gyromagnetic constant, distortion due to the modulation frequency is ignored, yielding the following model for the modulation-distorted lineshape, f:

$$f(B;d,\Gamma,B_m)=\mathrm{Im}\left(\frac{dB_m}{\alpha}\right), \tag{1}$$

where

$$\alpha=\frac{a^2}{2}\left(1+\sqrt{1-\left(\frac{B_m}{2a}\right)^2}\right)-\frac{B_m^2}{8} \tag{2}$$

and

$$a=B+j\Gamma. \tag{3}$$

Here, B is the applied magnetic field, j is the imaginary unit, and Im $(\cdot)$ represents the imaginary part of its argument.

Each scan is composed of M_n successive samples taken at uniform intervals across the field scan. The measured data for scan $n\in\{1,\ldots,R\}$ is then given by

$$Y_{i,n}=f(B_{i,n};d,\Gamma,B_{m,n})+\frac{N}{\sqrt{T_n/M_n}}\equiv f_{i,n}+\frac{N}{\sqrt{T_n/M_n}}, \tag{4}$$

where

$$B_{i,n}=\frac{i\Delta_{B,n}}{M_n-1}-\frac{\Delta_{B,n}}{2},\ i\in\{0,\ldots,M_n-1\}, \tag{5}$$

and N is additive white Gaussian noise with standard deviation σ_N. T_n is the time spent on scan n: $T_1+\cdots+T_R$ must equal T, the total time of the experiment. The penalty for spending less time on a given scan is to either increase the noise in each sample of the scan or to decrease the number of samples in the scan. Fig. 1 shows an example of two simulated equal-time scans with different modulation amplitudes and sweep widths.

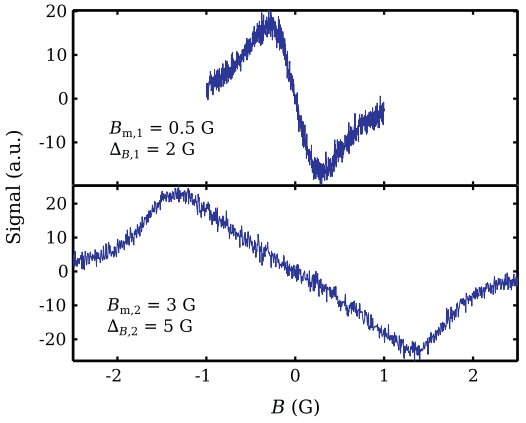

Fig. 1. Two equal-time ($T_1=T_2$) scans may be more informative than a single-scan. A HWHM linewidth of 0.4 G is depicted here, with $d=10$, $\sigma_N=1$, and $M_n=1024$.

Let $\vec{\theta}=[d,\Gamma,B_{m,1},\ldots,B_{m,R}]$ denote a list of $R+2$ unknown parameters. Once the scan parameters are selected, noisy measurements $\vec{Y}_n=[Y_{0,n},\ldots,Y_{M_{n-1},n}]$ are collected (either by simulation or by experiment), and the unknown linewidth is estimated by a weighted least-squares curve fit:

$$\hat{\vec{\theta}}=\underset{\vec{\theta}}{\mathrm{argmin}}\sum_{i,n}\frac{T_n}{M_n}(f_{i,n}-Y_{i,n})^2. \tag{6}$$

Here $\hat{\vec{\theta}}$ is the estimated value of $\vec{\theta}$.

2.2. Statistical analysis

The CRLB provides a lower bound on the standard deviation of an unbiased parameter estimator. Intuitively, if small changes in presumed parameter values cause a *small* change in the fit error of Eq. (6), then the estimation is easily corrupted by noise. Conversely, if small changes in presumed parameter values cause a *large* change in the fit error, then the estimation is more robust to noise. This intuition is formalized by the CRLB, which can be used as a tool for experiment design.

The CRLB is computed from the inverse of the Fisher information matrix, $\mathcal{I}$ (see [17], page 378). Each scan is described by a separate information matrix, $\mathcal{I}_n$. For the nth scan, let $p(\vec{Y}_n|\vec{\theta})$ be the probability density function of the data $\vec{Y}_n$ conditioned on parameters $\vec{\theta}$. Then the elements of the corresponding information matrix according to Eq. (4) are as follows:

$$\begin{aligned}(\mathcal{I}_n)_{k,l}&=-\mathrm{E}_{\vec{Y}_n}\left[\frac{\partial^2}{\partial\theta_k\partial\theta_l}\log(p(\vec{Y}_n|\vec{\theta}))\right]\\&=\frac{T_n}{2M_n\sigma_N^2}\mathrm{E}_{\vec{Y}_n}\left[\sum_i\frac{\partial}{\partial\theta_k}\frac{\partial}{\partial\theta_l}(Y_{i,n}-f_{i,n})^2\right]\\&=\frac{T_n}{M_n\sigma_N^2}\sum_i\left(\frac{\partial}{\partial\theta_k}f_{i,n}\right)\left(\frac{\partial}{\partial\theta_l}f_{i,n}\right).\end{aligned} \tag{7}$$

Here $\mathrm{E}_{\vec{Y}_n}[\cdot]$ denotes the expectation over $\vec{Y}_n$. The size of the information matrix, $\mathcal{I}_n$, is $(R+2)\times(R+2)$.

Fisher information from independent experiments is additive. When multiple scans are performed, the total information is the sum of the information from each scan:

$$\mathcal{I}=\sum_n\mathcal{I}_n. \tag{8}$$

The CRLB on the standard deviation of the estimated linewidth $\hat{\Gamma}$ is obtained from the Fisher information as follows:

$$\mathrm{CRLB}_{\hat{\Gamma}}(\vec{\theta};\Delta_{B,1},\ldots\Delta_{B,R},T_1,\ldots,T_R,\sigma_N)=\sqrt{(\mathcal{I}^{-1})_{2,2}}. \tag{9}$$

Given a range $[\Gamma_{\min},\Gamma_{\max}]$, the goal is to determine the number of scans, R, and the corresponding parameters $B_{m,1},\ldots,B_{m,R}$, $\Delta_{B,1},\ldots,\Delta_{B,R}$, $T_1,\ldots,T_R$ that minimize the average $\mathrm{CRLB}_{\hat{\Gamma}}$ across $[\Gamma_{\min},\Gamma_{\max}]$. To this end, for a candidate number of scans, R, and a fixed range $[\Gamma_{\min},\Gamma_{\max}]$, we exhaustively numerically search for the R modulation amplitudes, R sweep widths, and R scan times to minimize the average $\mathrm{CRLB}_{\hat{\Gamma}}$. For the sake of comparison, parameters for single-scan acquisition (i.e., $R=1$) were also optimized to minimize the average $\mathrm{CRLB}_{\hat{\Gamma}}$.

3. Material and methods

In this section, we describe the construction of oxygen-sensitive phantoms. We also outline the data acquisition protocols used for L-band oximetry.